Supplementary material

Quantitative reverse transcription PCR

RNA samples were extracted with phenol/chloroform and treated with RNase-free DNase I. RNA was reverse-transcribed using the SuperScript II reverse transcription kit (Invitrogen) and random hexamers. Quantitative real time PCR experiments were performed in triplicate using the LightCycler FastStart DNA Master SYBR Green I kit (Roche Applied Science). The $2^{-\Delta\Delta CT}$ method was used to calculate the relative expression levels. Each result was normalized to HPRT, Hypoxantine guanine phosphoribosyl transferase. As the minimum detectable change, we used a 2-fold expression difference and considered only expression differences equal to or higher than 2-fold as significant (as done previously in Bach et al., 2009).

Supplementary Figures legend

Supplementary Figure 1. Repercussion of ER stress and proteasomal inhibition on PrP aggregation in L929 fibroblasts. (A) L929 fibroblasts were treated with the indicated compounds for 16h (M: mock; MG: MG132; T: Tunicamycin; Th: Thapsigargin). Soluble (supernatant; S) and insoluble (pellet; P) fractions in postnuclear lysates were separated by solubility assay, deglycosylated with PNGaseF, and subjected to immunoblotting and PrP detected with mAb 4H11. Induction of ER stress was confirmed with antibodies for Grp78/BiP. Equal protein loading was verified with actin. The doublet bands for deglycosylated PrP most likely originate from incomplete deglycosylation (see also Fig. 1B). (B) Desitometric evaluation of immunoblots with L929 cells (each performed in triplicate). Bars represent amount of insoluble PrP expressed as percentage pellet found in mock-treated cells. Proteasomal impairment by MG132 treatment does not significantly alter transcription of *prnp* gene. **(**C) Quantitative *Prnp* expression levels in L929 fibroblasts in mock- or MG132-treated cells were determined by real time PCR. All results were normalized to HPRT (hypoxantine guanine phosphoribosyl transferase) expression levels. For triplicate experiments, the standard deviation is shown for each gene. The *y* axis denotes the comparative gene expression levels. *Bars* represent mean values ± S.D. ($n = 4$).

Supplementary Figure 2. Proteasomal inhibitor Lactacystin increases surface expression of PrP^{c}. FACS analysis in non-permeabilized HpL3-4 (over-expressing PrP) and L929 cells shows significant higher surface localization in Lactacystin-treated cells (open lines) compared to mock-treated cells (grey curves).

Supplementary Figure 3. ER stress and proteasomal impairment lead to increased accumulation of PrP^{Sc} in prion-infected cells. (A) The amount of PrP^{Sc} in HpL-22L and L929-22L cells and treated

with Lactacystin (Lac) or Thapsigargin (Th) was compared to the one in mock-treated cells (M). Immunoblots show total PrP- (-PK) and PrP^{Sc}-content (+PK) in postnuclear lysates probed with mAb 4H11. Lowest panels show actin loading controls. (B) Densitometric evaluation of at least two independent experiments performed in triplicate confirms significant increase of PrP^{Sc} in compound-treated compared to mock-treated cells ($p \leq 0{,}005$).

Suppl. Figure 1

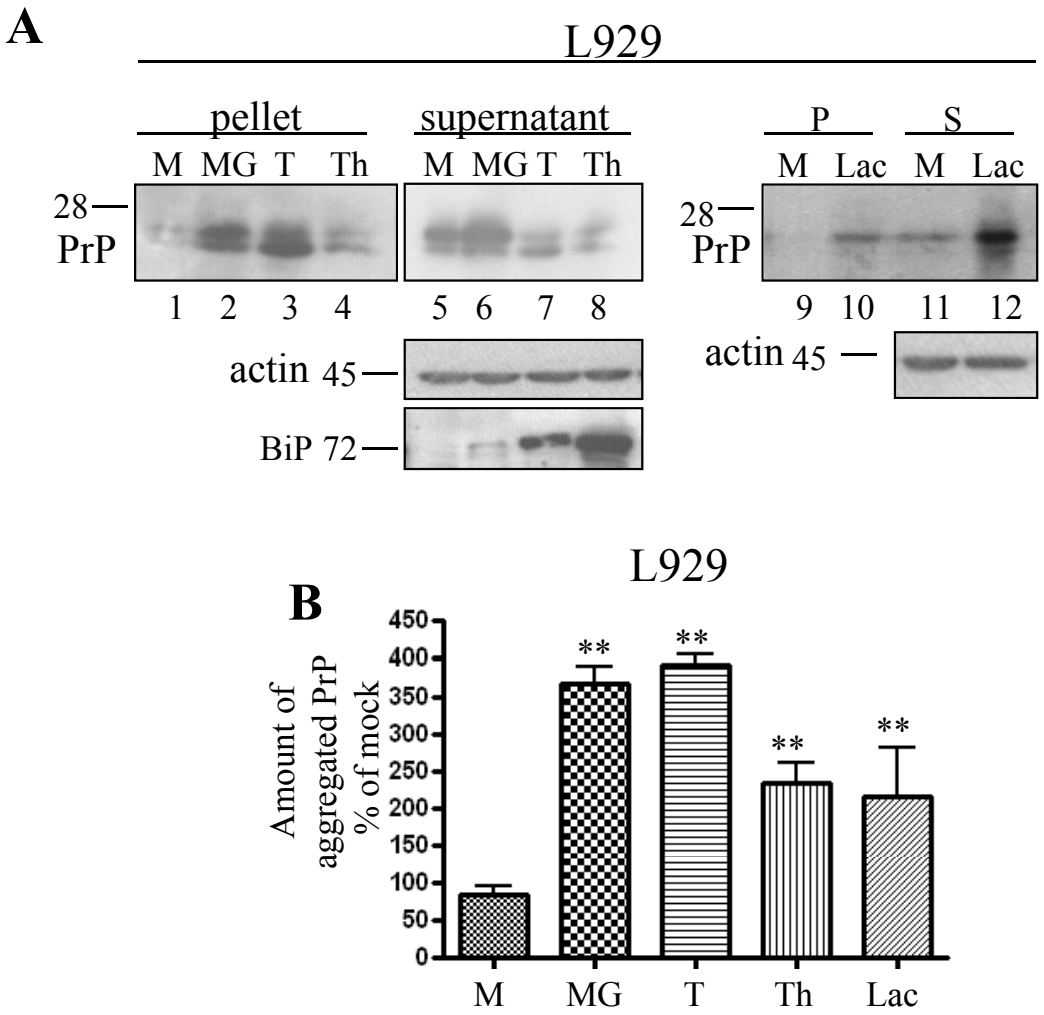

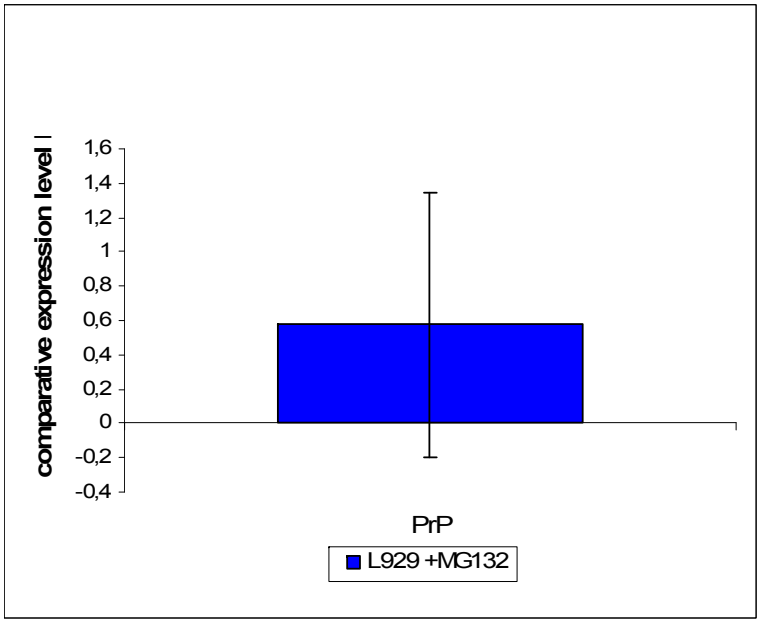

Supplementary figure 2

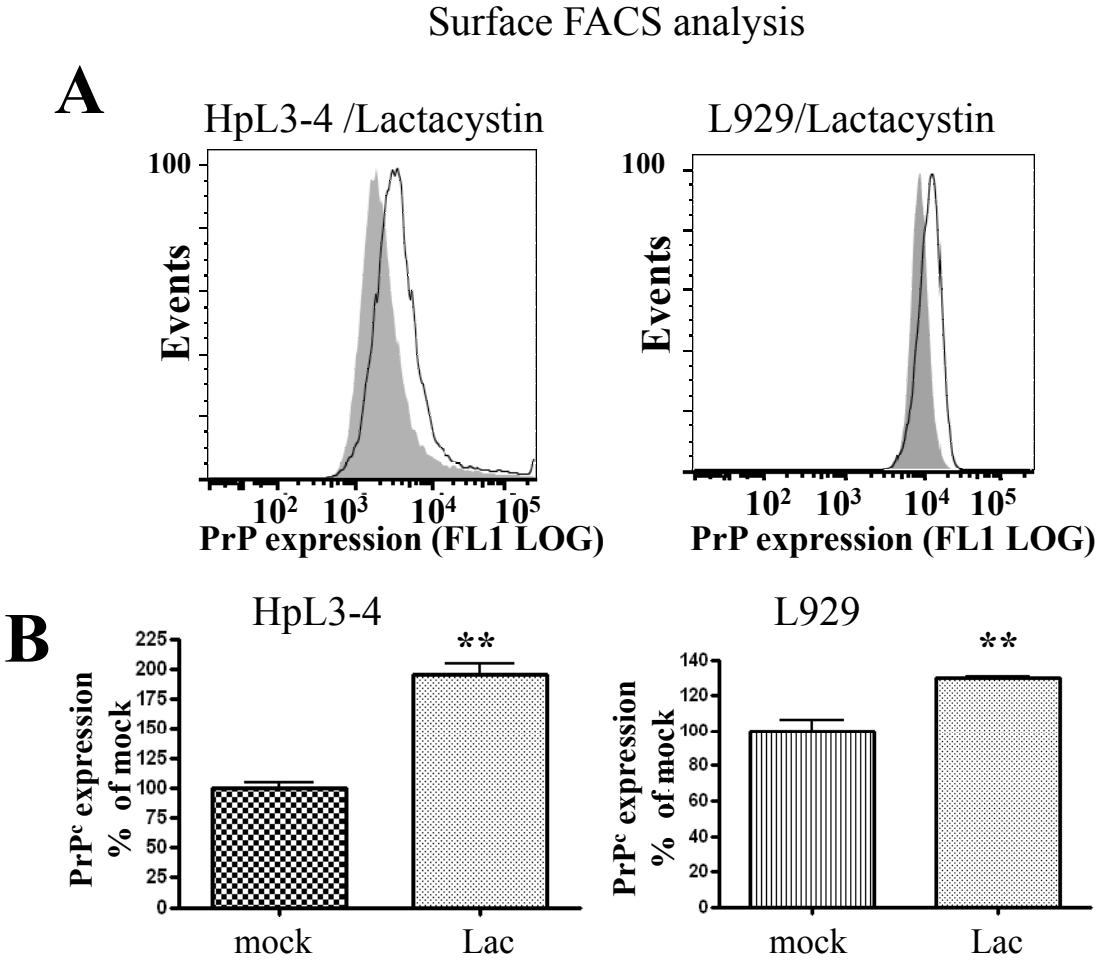

Suppl. Figure 3